NANO LETTERS

pubs.acs.org/NanoLett Letter

Adenoviral Vector for Enhanced Prostate Cancer Specific Transferrin Conjugated Drug Targeted Therapy

Jing Peng,[#] Kangkang Liu,[#] Lin Cao,[#] Dengyi Duan, Guodong Song, Shuang Liu, Lining Wang, Jianmin Li, Xuening Zhang, Kai Huang, Yang Zhao,[*] Yuanjie Niu,[*] and Gang Han[*]

Cite This: https://doi.org/10.1021/acs.nanolett.2c00931 Read Online

ACCESS | Metrics & More | Article Recommendations | Supporting Information

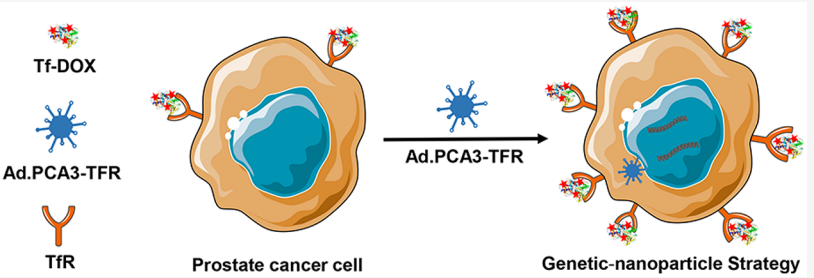

ABSTRACT: Prostate cancer (PCa) is one of the leading causes of death for men worldwide. Unlike some other types of cancer, there is a lack of targeted therapy for prostate cancer patients that can kill cancer cells but do much less damage to the normal tissue. In this paper, we report on an adenoviral vector enhanced prostate cancer specific transferrin conjugated drug targeted therapy. In particular, a functional PCa-specific gene probe is introduced to drive and up-regulate the transferrin receptor expression on the PCa via adenoviral vector. As a result, significantly enhanced accumulation of nanoscale transferrin-doxorubicin (Tf-DOX) protein drug conjugates and concomitant notably elevated PCa tumor inhibition are observed. This conceptual strategy provides the proof-of-concept for the targeted therapy of PCa that is highly desired but not yet developed.

KEYWORDS: *gene probe, transferrin conjugated drug delivery, prostate cancer, targeted therapy*

Prostate cancer (PCa) is one of the most common malignancies in men worldwide. According to the National Cancer Institute (NCI), this type of cancer affects one in every nine men and is the second most common cause of cancer-related death in the U.S.[1,2] In particular, advanced and recurrent PCa patients are considered to be incurable.[3] The only clinical choice for the such patients is extensive chemotherapy and radiation therapy that are extremely invasive and have severe side-effects on normally functioning organs and tissues, and the median period of survival once starting such treatment is only 1−3 years.[4−6] In contrast, targeted therapies that can kill cancer cells but do much less damage to the normal tissue are becoming an important treatment method and lead to a notably better prognosis for certain types of cancers.[7,8] Yet, none of these targeted therapies has been well established for PCa patients. Traditional PSMA-targeted approach depends on the intrinsic expression level of the target antigens of the tumor itself. However, since many prostate cancer antigens, including PSMA, are very heterogeneous, the treatment outcome is unsatisfactory for certain patients.[9] In this paper, we report on a new PCa target therapy via a genetic-nanoparticle approach. In such an approach, the target protein gene can be introduced into a tumor through adenovirus vector to significantly increase the expression of the target gene in the tumor, thus ameliorating the heterogeneity and ultimately enhancing the drug targeting.

In particular, transferrin (Tf)-conjugated drug delivery systems have been explored clinically as an emerging target therapy method.[10] This is due to the up-regulated levels of transferrin receptor (TfR) expression in certain types of cancers as well as to the reported on Tf's unique recycling pathways.[11,12] For example, Tf-CRM107 is a covalent conjugate Tf protein to a diphtheria toxin with a point mutation (CRM107), the latter of which diminishes the native toxin binding.[13,14] In its clinical trials, the Tf-CRM107 has proved its tumor response in patients with malignant refractory brain tumors without severe neurologica or systemic toxicity.[14] Moreover, doxorubicin (DOX) has also been conjugated to Tf protein.[15] Such Tf-DOX conjugate has also been proven to be effective in improving therapeutic outcomes in some types of malignancies.[16,17] However, despite these advances, the current

Received: March 8, 2022
Revised: May 2, 2022

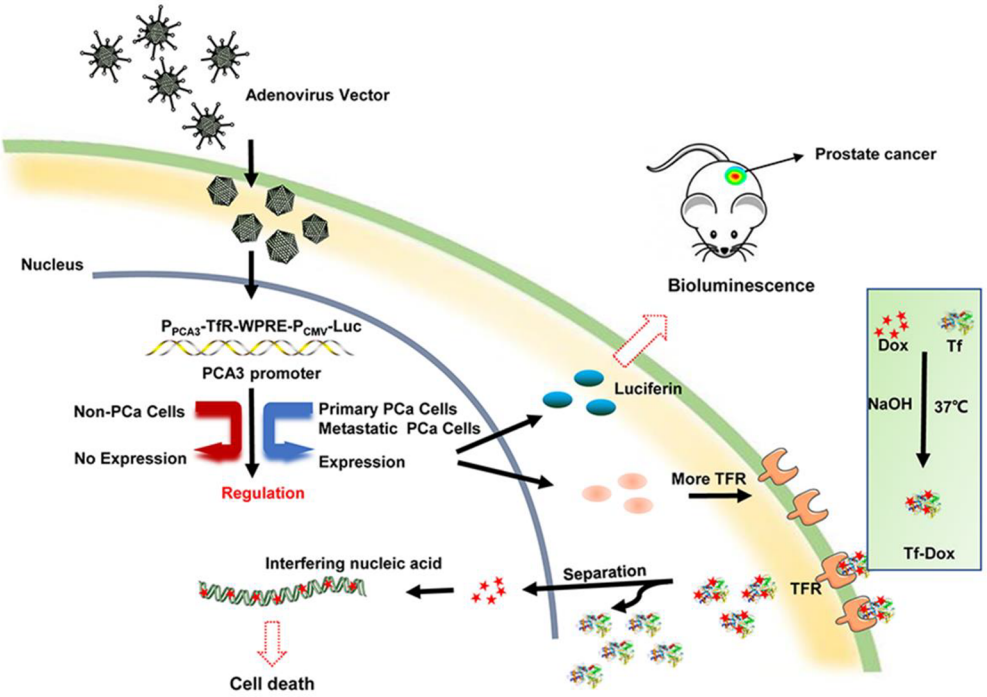

Figure 1. Bioluminescence imaging and targeted precision therapy. The P_{PCA3}-TFR-TfR-Luc gene carried by adenovirus can selectively overexpress the TfR protein and luciferin in prostate cancer cells. Increased TfR enhances the uptake of Tf-DOX nanoparticles and thus increases antitumor effects.

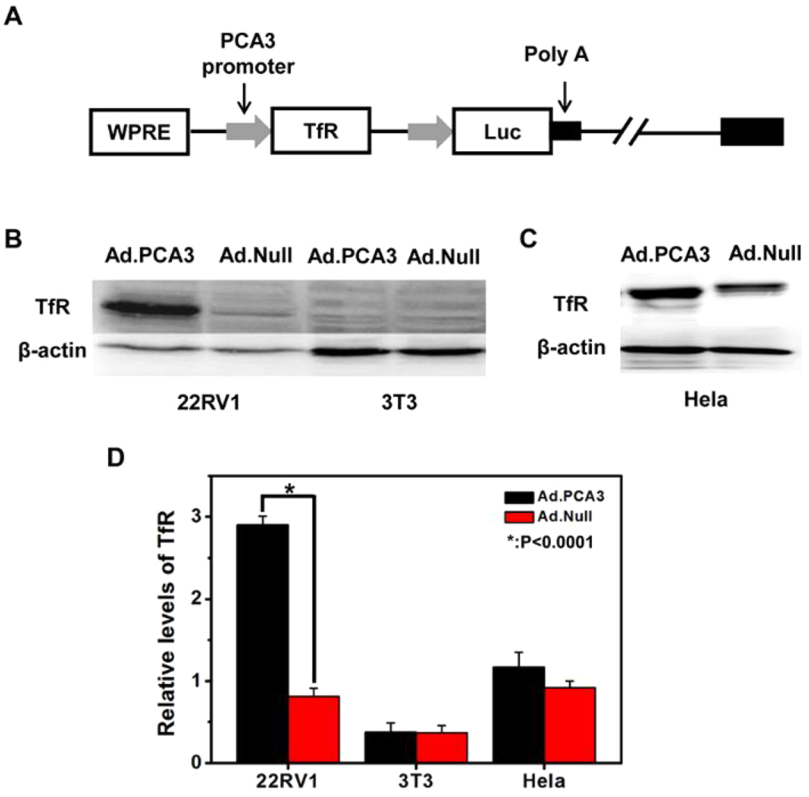

Figure 2. Construction and characterization of Ad.PCA3 probe. (A) Scheme of the recombinant adenoviral vectors driven by the DD3 promoter and WPRE regulatory element. (B, C) Western blot analysis of TfR expression in prostate cancer cells (22RV1), normal cells (3T3), and nonprostate tumor cells (Hela) 24 h after infection with equal amount of Ad.PCA3 and Ad.Null. (D) Relative densimetry of TfR protein in various cell lines infected either with or Ad.Null, as determined by semiquantitative Western blot. The error bars represent data from three independent experiments.

https://doi.org/10.1021/acs.nanolett.2c00931
Nano Lett. XXXX, XXX, XXX−XXX

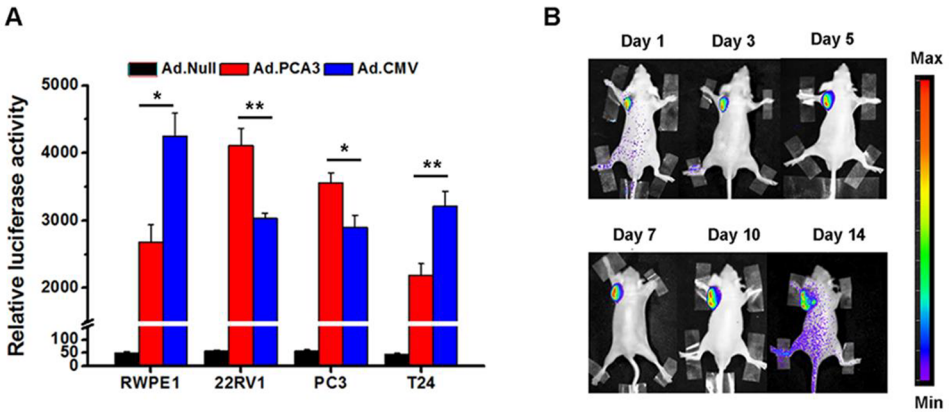

Figure 3. Bioluminescence *in vitro* and *in vivo*. (A) Biolominescence intensity of various cell lines at 24 h posttransfections of Ad.PCA3. Ad.CMV and Ad.Null served as the controls. (B) Dynamic optic imaging of 22RV1-bearing mice at different time points postintratumoral injection of Ad.PCA3.

sensitivity, specificity, and efficiency are still not satisfactory for the targeting therapy of PCa tumor. This is due to the multifocality and heterogeneity nature of PCa tissues.[18−20] For example, the expression of TfR varies in different PCa cell lines and even between every single cell of the same cell line, which reveals that the individual heterogeneity of TfR among PCa patients may cause the failure of TfR targeted therapy.[21] Therefore, providing an abundant level of Tf-TfR binding in PCa would be a feasible way to use Tf-based drug delivery systems for targeted therapies of PCa.[22]

To this end, a functional PCa-specific gene probe is introduced via an adenoviral vector to enhance the tumor targeting of the Tf protein drug conjugates. In brief, first, the PCa-specific gene probe is designed as follows. In particular, the PCa-specific PCA3 promoter, also known as differential display 3 (DD3), was successfully inserted into the upstream of the luciferase (Luc) reporter and the TfR expression cassettes to achieve the selective expression in PCa cells.[23] On the basis of its ability to increase gene transcription, the woodchuck hepatitis virus posttranscriptional regulatory element (WPRE) enhancer was further incorporated into the PCA3 promoter-driven gene probe. The Luc gene was inserted as an imaging readout for the gene expression in the tumors. The TfR gene was incorporated into the gene probe to up-regulate the TfR expression on the PCa cell membrane, thus enhancing the PCa specific Tf protein conjugated drug tumor targeting (Figure 1). Then the recombinant fragment was then packaged into an adenoviral vector. A representative scheme for the resulting adenoviral vector, Ad.P_{PCA3}-TfR-WPRE-P_{CMV}-Luc (Ad.PCA3 in brief), was presented (Figure 2A). To investigate the specific expression of Ad.PCA3, an adenovirus vector package without a recombination gene (Ad.Null) was constructed as a negative control, while Ad.P_{CMV}-Luc (Ad.CMV) was set up as a positive control, where the expression of a Luc reporter was driven by a constitutive cytomegalovirus (CMV) promoter.

The tumor-targeting ability of Ad.PCA3 was further evaluated by comparing the expression level of the TfR protein in various cell lines. As a high-malignancy and well established *in situ* recurrent human PCa model, the PCa 22RV1 cancer cell was used in this study.[24] As shown in Figure 2B, no obvious expression of TfR was present in Ad.PCA3 and Ad.Null treated normal 3T3 cells, whereas Ad.PCA3 treated 22RV1 cells had an overexpression of the TfR protein (Figure 2B). In human cervical cancer Hela cells, TfR protein in Ad.PCA3 treated Hela cells was slightly higher than that in Ad.Null (Figure 2C). However, compared to Ad.Null groups, only the overexpression of TfR protein in Ad.PCA3 treated 22RV1 cells was statistically significant, confirming that the prepared gene probe can target such PCa cells with high specificity (Figure 2D).

To evaluate the expression level of the Luc reporter, the bioluminescence intensities of several different cell lines, including the partial androgen-dependent PCa cell line (22RV1), the androgen-independent PCa cell line (PC3), the bladder cancer cell line (T24), and a normal prostate cell line (RWPE1), were quantitatively analyzed. As shown in the figure, 22RV1 cells infected with Ad.PCA3 emitted significantly higher bioluminescence intensity than those treated with Ad.CMV. When compared to Ad.CMV, slightly increased bioluminescence was also observed in the Ad.PCA3-treated PC3 cells. The bioluminescence intensity in Ad.PCA3-treated RWPE1 cells and T24 cells was lower than that in the same cell lines treated with Ad.CMV instead. Meanwhile, none of the Ad.Null treated cell lines showed obvious luminescence (Figure 3A). The results indicated that the constructed gene probes exhibited high specificity for PCa cells but had weak activity regarding non-PCa tumor cells and normal cells.

Next, to assess the *in vivo* effectiveness of the proposed diagnostic strategy mediated by the PCA3 promoter, ten 22RV1-bearing mice were allowed to grow tumors until the visible tumor size reached 0.5 cm diameter. Then dynamic optic imaging during an observation time of 14 d was performed to monitor the natural development and random metastasis of PCa after the intratumoral injection of Ad.PCA3. When in the prone position, the bioluminescence signals derived from Ad.PCA3 were only visualized and centralized at the tumor site on the left shoulder of mice on the first day postadministration, with clear boundaries between the tumor tissue and surrounding tissue. Subsequently, tumor bioluminescence intensity enhanced progressively over time and became enlarged in dimensions in accordance to the growing tumor. The bioluminescence intensity of tumors reached a peak at 7 to 10 days postinjection (Figure 3B; Figure S1). Except for in the supine position, in all optical images taken at different postinjection time points, no bioluminescence was found in major organs including liver, spleen, kidney, bladder, lungs, and heart, or in the rest of the body (Figure S2). The above results showed that Ad.PCA3 probe can be used as an

https://doi.org/10.1021/acs.nanolett.2c00931
Nano Lett. XXXX, XXX, XXX−XXX

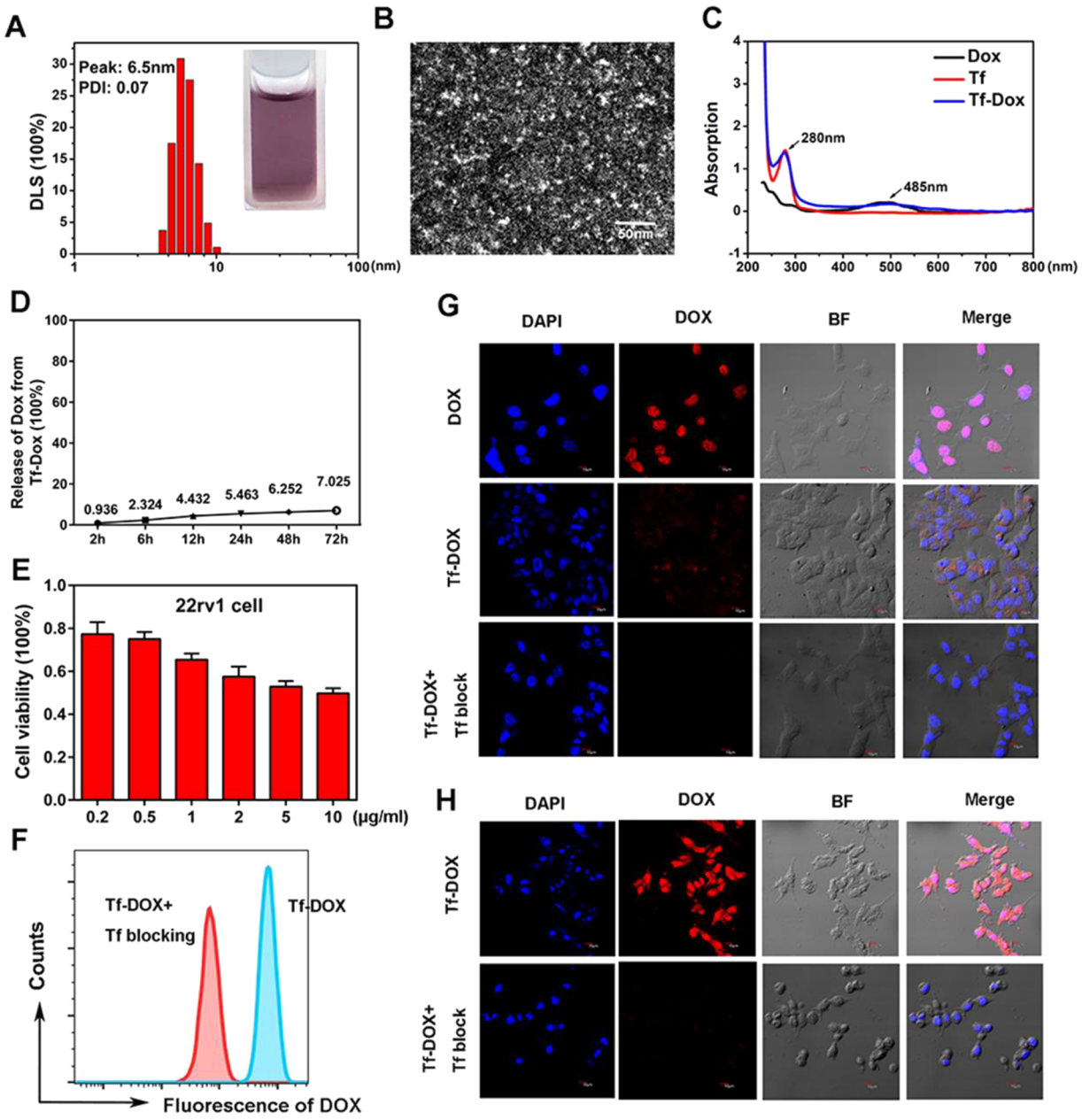

Figure 4. Characterization of Tf-DOX nanoparticles. (A) Appearance and DLS. (B) TEM. (C) UV absorption curve of Tf-DOX nanoparticles. (D) Release of DOX from Tf-DOX at different time in PBS. (E) MTT cell viability experiment of the different concentrations of Tf-DOX on 22RV1 cells at 48 h. (F) Flow cytometric analysis of Tf-DOX. (G, H) Tf protein competition inhibition experiment at 1 h and 24 h by CLSM.

effective bioluminescence imaging tool for monitoring the growth of PCa with no background fluorescence.

Because of the silent but prevalent metastasis of PCa, detection of metastasized tumor sites has proven to be more difficult than that for the primary tumor. To demonstrate the capacity of our constructed probe in the early detection and diagnosis of advanced stage PCa, we further investigated the bioluminescence imaging ability of our probe in metastatic tumor tissue. After intratumoral injection of Ad.PCA3 into the living tumor-bearing mice, we monitored the development of tumors within small animals via optical imaging. All 22RV1-bearing mice showed clear bioluminescence in tumor areas. Remarkably, in one of the mice, which was at 26 days postinjection, an additional bioluminescence signal was detected in the spinal region near the neck (Figure S3). The oval-shaped signal had clear boundaries and demonstrated medium intensity in the blue spectrum. No bioluminescence was found in other parts of the body, and the physical appearance of the mouse was normal compared to other mice. According to the position of the fluorescent spot, we performed surgical anatomy on the mouse to obtain micro-lesion. The mouse was sacrificed, and surgery exploration revealed that the region with bioluminescence had pathological fraction with irregular mass and indistinguishable border with the surrounding vertebra (Figure S4A). The abnormal tissue was dissected for hematoxylin/eosin (HE) staining and was confirmed to be bone metastasis. Immunohistochemical analysis (IHC) for PSMA and Ki67 proteins was performed to confirm the PCa specificity and cellular viability of metastasis (Figure S4B). The findings showed that our method

https://doi.org/10.1021/acs.nanolett.2c00931
Nano Lett. XXXX, XXX, XXX−XXX

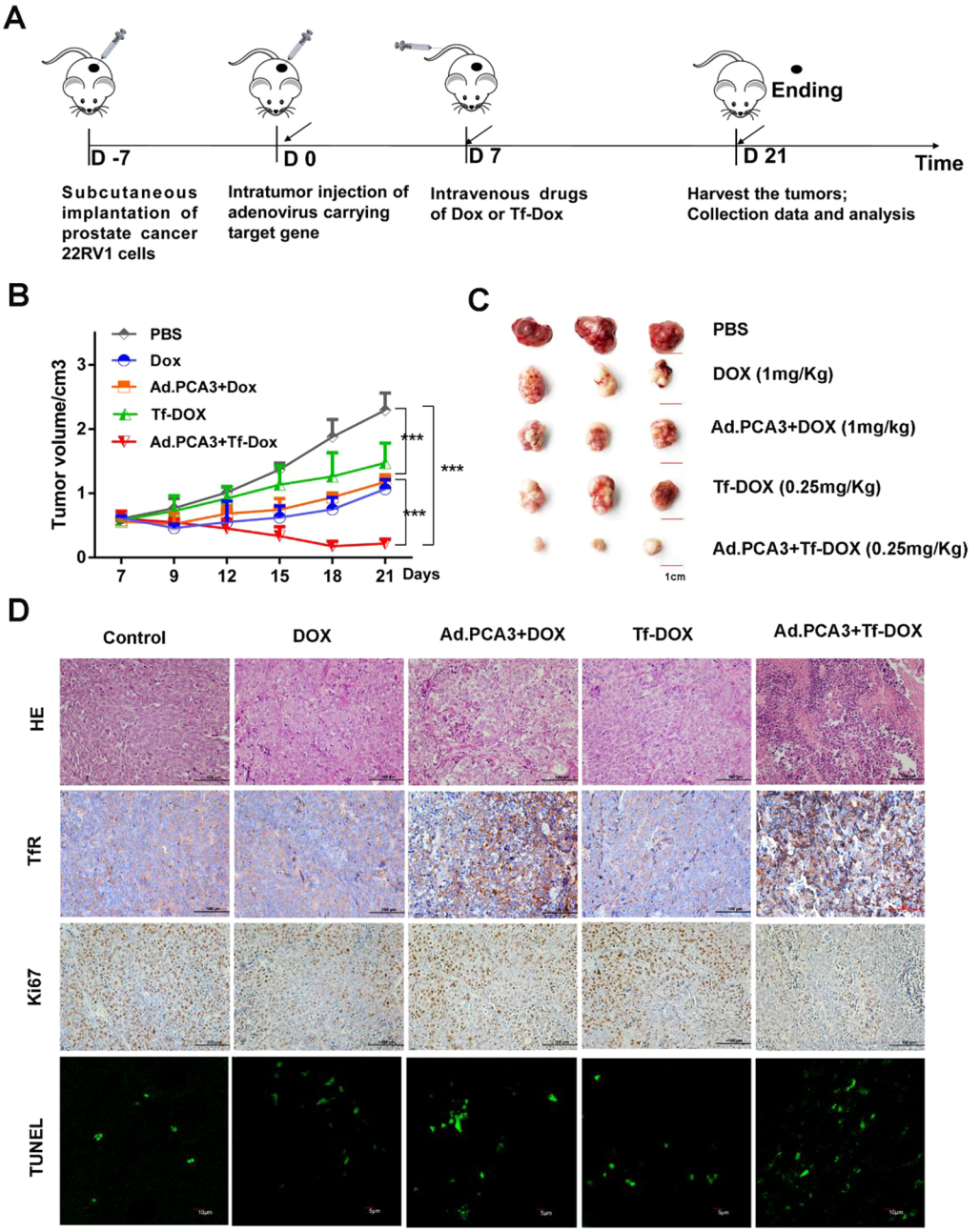

Figure 5. Antitumor effect *in vivo*. (A) Schematic diagram of *in vivo* animal experiment. (B) Growth curve of the tumor was detected from the 7th day to the end of the 21st day. The volume of the tumor was calculated according to the following formula: $V = a \times b^2/2$ where a and b were the longest and shortest diameters of tumor. (C) Harvesting the final tumors and photograph. (D) HE staining, IHC of TFR and Ki67, and TUNEL staining.

has therapeutic potential in regard to the early micrometastases of PCa.

The specific overexpression of TfR in PCa by our dual functional gene expression cassette probe can potentially improve the delivery efficiency and tumor targeting of the noted Tf-TfR metabolic pathway. Therefore, we further evaluated the synchronous antitumor effect of Tf protein and chemotherapeutic drug conjugates by combining with Ad.PCA3 probe. Doxorubicin (DOX) is a broad-spectrum chemotherapy, which is used in the treatment of a variety of cancers including PCa. In our study, Tf-DOX was synthesized directly by one-step method and used to evaluate the therapeutic effect on PCa. The DOX was loaded within the Tf protein by noncovalent hydrophobic interactions. TEM and DLS showed that the average size of Tf-DOX nanoparticles was around 6 nm (Figure 4A,B).

By continuously monitoring the change of particle size for a week, we found that the particle size did not change distinctly, which confirmed that the Tf-DOX nanoparticles we synthesized possessed good stability (Figure S5). The UV characteristic absorption peak of Tf-DOX confirmed the successful binding of DOX and Tf, and the peak intensity was used to measure the concentration of DOX binding in Tf-DOX (Figure 4C). The release curve of DOX shed from Tf-DOX nanoparticles at different times was monitored, showing that DOX was slightly released over time, which indicated that the

https://doi.org/10.1021/acs.nanolett.2c00931
Nano Lett. XXXX, XXX, XXX−XXX

connection between Tf protein and DOX was reliable (Figure 4D). In addition, MTT cell viability experiments confirmed that Tf-DOX nanoparticles had a concentration-dependent killing effect on PCa 22RV1 cells *in vitro* (Figure 4E).

To further confirm that the successful synthesis of Tf-DOX and the cellular uptake of nanoparticles were mediated by TfR receptors, a Tf protein competition inhibition experiment was performed. Flow cytometry (FCM) analysis showed that after Tf protein blocking, the fluorescence of Tf-DOX was dramatically inhibited in 22RV1 cells, while the fluorescence of DOX was unchanged after Tf blocking (Figure 4F; Figure S6). The confocal laser scanning microscope (CLSM) showed that DOX alone quickly gathered in the nucleus in 1 h after cocultivation, while the DOX in the Tf-DOX group was mainly concentrated in the cytoplasm and not seen in the nucleus at 1 h time point. When Tf protein was added to block the TfR receptor on the cell surface in advance, DOX was almost not seen in the cell, which meant that the uptake of Tf-DOX nanoparticles was regulated by TfR-mediated endocytosis (Figure 4G). Then 24 h after coculture, we found that a large amount of DOX was released from Tf-Dox and could be seen to be accumulated in the nucleus (Figure 4H, Figure S7). Meanwhile, the Tf protein blocked group still maintained low DOX uptake. Therefore, these results confirmed that our synthesized Tf-DOX nanoparticles can be taken up by PCa cells through the Tf-TfR system.

Next, the half-lives of Tf-DOX and free DOX after intravenous injection were studied, and the results showed that the half-life of Tf-DOX (0.63 h) was 8-times longer than that of the free DOX (0.07 h) (Figure S8). The organ distribution of Tf-DOX was studied via *ex vivo* fluorescence imaging at different time points after Tf-DOX injection, and the results showed that Tf-DOX had negligible accumulation in the major organs at 24 h after injection (Figure S9). Moreover, we further demonstrated that Tf-DOX had a significant accumulation in the tumor of the mice, and the accumulation was more in our Ad.PCA3 treated group than the control group (Figure S10). Furthermore, after Tf-DOX treatment intravenously injected into the mice, the tumors were harvested and fluorescence observation of DOX was performed, and the results showed that the fluorescence of DOX was found both at the margins of the tumor as well as in the deep interior after our Ad.PCA3 treatment (Figure S11). These results exhibited excellent tumor targeting and negligible body accumulation of Tf-DOX nanoparticles in regard to our gene-nanoparticle strategy.

Then we verified the antitumor effect of our gene probe combined with tumor targeting Tf-DOX nanoparticles on PCa *in vivo*. The experiments were carried out in 22RV1 tumor-bearing nude mice, divided into five groups: (1) PBS control, (2) DOX (1 mg/kg), (3) Ad.PCA3+DOX (1 mg/kg), (4) Tf-DOX (0.25 mg/kg), (5) Ad.PCA3+Tf-DOX (0.25 mg/kg). On the seventh day after the tumor was planted subcutaneously, intratumoral injection of adenovirus vector was performed, which was a commonly used administration route in the clinical practices of gene therapy due to its high efficacy and favorable biosafety and biodistribution.[25−27] For example, patients with malignant glioma have been reported to have undergone intratumoral local injection of oncolytic adenovirus to treat recurrent lesions.[28] Since the complete expression of the conventional adenovirus vector plasmid is strongest in about a week, 7 days after adenovirus injection, mice in each group were given intravenous injection of DOX or Tf-DOX treatment. The mice were sacrificed on the 21st day, and tumors and various tissues and organs were collected for analysis (Figure 5A).

Compared with the PBS control, intravenous injection of DOX alone has a slight inhibitory effect on tumor growth, which is similar to the combined Ad.PCA3 group. This indicates that the Ad.PCA3 probe itself has no significant effect on tumor growth. To verify that our probe can achieve a better antitumor effect at a low dose of drug concentration by increasing the aggregation and uptake of nanoparticles at the tumor site, we used Tf-DOX nanoparticles whose DOX content was only a quarter of that of the DOX alone group to treat tumors. At this low dose, the inhibitory effect of Tf-DOX nanoparticles, which is actively targeted to tumors, was similar to that of DOX alone, indicating that the antitumor improvement of active targeting nanoparticles alone is not enough. Remarkably, the combination of Ad.PCA3 gene probe and Tf-DOX nanoparticles showed a significant inhibitory effect on tumor growth, even at a low DOX concentration (Figure 5B,C). The results supported that our gene-nano system can effectively enhance the tumor targeting and further improve the antitumor efficacy even at low drug concentrations.

Then we performed immunohistochemical (IHC) analysis of TfR expression in different groups. The tumor tissue TfR of Ad.PCA3+DOX and Ad.PCA3+Tf-DOX groups showed significantly high expression, which indicated that our gene probe was successfully expressed in *in vivo* tumor. Meanwhile, the intratumor Ki67 level of Ad.PCA3 group was significantly lower than that of the other groups, while the TUNEL positive cells were significantly higher (Figure 5D). These results indicated that the gene probe combined with nanomedicine can greatly inhibit tumor growth by decreasing cell proliferation and promoting apoptosis.

Finally, to verify the biosafety of Ad.PCA3 gene probe combined with Tf-DOX nanoparticles strategy, we performed HE staining on the main organs of Ad.PCA3+Tf-DOX group and control mice. HE results showed that intratumoral injection of adenovirus vector did not cause significant damage to the major organs of mice including the heart, liver, spleen, lung, kidney, and brain (Figure S12). These results suggested a good biosafety of our gene-nano strategy.

In summary, we successfully validated that PCA3 promotor-based gene probe can be used for PCa-specific targeted therapy. The optical images performed with the gene probe *in vivo* demonstrated a strong and long-lasting bioluminescence signal exclusively at the tumor areas with clear boundaries separating tumors from the surrounding tissue, and the signal was changing in dimensions in accordance to the tumor growth. The crucial dual design of this gene probe, combing a therapeutic TfR gene, can enhance Tf-based nanoscale protein drug conjugate targeted theranostics while reducing their administration doses, thus providing a promising general strategy for further augmenting efficacy and biosafety of nanomedicine. Moreover, as an anticipatable application of the gene probe in a clinical setting, the results indicated that this strategy based on PCA3 promoter can be expanded to specifically overexpress a wide variety of other functional proteins in PCa with great specificity and efficiency, thereby having great potential for further studies and clinical translation.

https://doi.org/10.1021/acs.nanolett.2c00931
Nano Lett. XXXX, XXX, XXX−XXX

■ ASSOCIATED CONTENT

Supporting Information

The Supporting Information is available free of charge at https://pubs.acs.org/doi/10.1021/acs.nanolett.2c00931.

Detailed experimental materials and methods; additional results for quantifying fluorescence value of Luc in tumor cells; dynamic optic imaging of tumors in supine position of mice; dynamic optic imaging of suspected lesions in thoracic vertebrae of mice; surgery exploration of primary PCa xenograft and pathology; stability and reliability of Tf-DOX; uptake of DOX in 22RV1 cells; uptake of Tf-DOX by lysosome; blood half-life, organ distribution, tumor targeting, tumor infiltration, and biosafety of Tf-DOX (PDF)

■ AUTHOR INFORMATION

Corresponding Authors

Gang Han − *Biochemistry and Molecular Biotechnology, University of Massachusetts Chan Medical School, Worcester, Massachusetts 01605, United States;* orcid.org/0000-0002-2300-5862; Email: gang.han@umassmed.edu

Yuanjie Niu − *Tianjin Institute of Urology and Department of Urology, The Second Hospital of Tianjin Medical University, Tianjin 300211, China*; Email: niuyuanjie@tmu.edu.cn

Yang Zhao − *Department of Radiology, The Second Hospital of Tianjin Medical University, Tianjin 300211, China; Tianjin Institute of Urology, The Second Hospital of Tianjin Medical University, Tianjin 300211, China; Biochemistry and Molecular Biotechnology, University of Massachusetts Chan Medical School, Worcester, Massachusetts 01605, United States*; Email: yang.zhao@tmu.edu.cn

Authors

Jing Peng − *Department of Radiology, The Second Hospital of Tianjin Medical University, Tianjin 300211, China; Biochemistry and Molecular Biotechnology, University of Massachusetts Chan Medical School, Worcester, Massachusetts 01605, United States*

Kangkang Liu − *Tianjin Institute of Urology and Department of Urology, The Second Hospital of Tianjin Medical University, Tianjin 300211, China*

Lin Cao − *Department of Radiology, The Second Hospital of Tianjin Medical University, Tianjin 300211, China*

Dengyi Duan − *Department of Radiology, The Second Hospital of Tianjin Medical University, Tianjin 300211, China*

Guodong Song − *Department of Gastroenterology, The Second Hospital of Tianjin Medical University, Tianjin 300211, China*

Shuang Liu − *Department of Radiology, The Second Hospital of Tianjin Medical University, Tianjin 300211, China*

Lining Wang − *Tianjin Institute of Urology, The Second Hospital of Tianjin Medical University, Tianjin 300211, China*

Jianmin Li − *Tianjin Institute of Urology, The Second Hospital of Tianjin Medical University, Tianjin 300211, China*

Xuening Zhang − *Department of Radiology, The Second Hospital of Tianjin Medical University, Tianjin 300211, China*

Kai Huang − *Biochemistry and Molecular Biotechnology, University of Massachusetts Chan Medical School, Worcester, Massachusetts 01605, United States*

Complete contact information is available at: https://pubs.acs.org/10.1021/acs.nanolett.2c00931

Author Contributions

#J.P., K.L., and L.C. contributed equally to this work.

Notes

The authors declare no competing financial interest.

■ ACKNOWLEDGMENTS

This work was supported by National Natural Science Foundation of China (Grant Nos. 91959114, 81872106), Natural Science Foundation of Tianjin (19JCZDJC33900, 20JCJQJC00270), and Scientific and Technological Research Program of Tianjin Municipal Education Commission (2019ZD025). G.H. was exclusively supported by the start-up fund of University of Massachusetts.

■ REFERENCES

(1) Siegel, R. L.; Miller, K. D.; Jemal, A. Cancer statistics, 2020. *CA: a cancer journal for clinicians* **2020**, *70* (1), 7−30.

(2) Hoffman, R. M. Clinical practice. Screening for prostate cancer. *New England journal of medicine* **2011**, *365* (21), 2013−2019.

(3) Sandhu, S.; Moore, C. M.; Chiong, E.; Beltran, H.; Bristow, R. G.; Williams, S. G. Prostate cancer. *Lancet* **2021**, *398* (10305), 1075−1090.

(4) Petrylak, D. P.; Tangen, C. M.; Hussain, M. H.; Lara, P. N., Jr.; Jones, J. A.; Taplin, M. E.; Burch, P. A.; Berry, D.; Moinpour, C.; Kohli, M.; et al. Docetaxel and estramustine compared with mitoxantrone and prednisone for advanced refractory prostate cancer. *New England journal of medicine* **2004**, *351* (15), 1513−1520.

(5) Zaorsky, N. G.; Harrison, A. S.; Trabulsi, E. J.; Gomella, L. G.; Showalter, T. N.; Hurwitz, M. D.; Dicker, A. P.; Den, R. B. Evolution of advanced technologies in prostate cancer radiotherapy. *Nature reviews. Urology* **2013**, *10* (10), 565−579.

(6) Chang, A. J.; Autio, K. A.; Roach, M., 3rd; Scher, H. I. High-risk prostate cancer-classification and therapy. *Nature reviews. Clinical oncology* **2014**, *11* (6), 308−323.

(7) Perez-Herrero, E.; Fernandez-Medarde, A. Advanced targeted therapies in cancer: Drug nanocarriers, the future of chemotherapy. *European journal of pharmaceutics and biopharmaceutics: official journal of Arbeitsgemeinschaft fur Pharmazeutische Verfahrenstechnik e.V* **2015**, *93*, 52−79.

(8) Zafar, A.; Wang, W.; Liu, G.; Wang, X.; Xian, W.; McKeon, F.; Foster, J.; Zhou, J.; Zhang, R. Molecular targeting therapies for neuroblastoma: Progress and challenges. *Medicinal research reviews* **2021**, *41* (2), 961−1021.

(9) Sheehan, B.; Guo, C.; Neeb, A.; Paschalis, A.; Sandhu, S.; de Bono, J. S. Prostate-specific Membrane Antigen Biology in Lethal Prostate Cancer and its Therapeutic Implications. *European urology focus* **2021**, DOI: 10.1016/j.euf.2021.06.006.

(10) Nogueira-Librelotto, D. R.; Codevilla, C. F.; Farooqi, A.; Rolim, C. M. Transferrin-Conjugated Nanocarriers as Active-Targeted Drug Delivery Platforms for Cancer Therapy. *Current pharmaceutical design* **2017**, *23* (3), 454−466.

(11) Zhao, Y.; Peng, J.; Li, J.; Huang, L.; Yang, J.; Huang, K.; Li, H.; Jiang, N.; Zheng, S.; Zhang, X.; et al. Tumor-Targeted and Clearable Human Protein-Based MRI Nanoprobes. *Nano Lett.* **2017**, *17* (7), 4096−4100.

(12) Li, H.; Qian, Z. M. Transferrin/transferrin receptor-mediated drug delivery. *Medicinal research reviews* **2002**, *22* (3), 225−250.

(13) Weaver, M.; Laske, D. W. Transferrin receptor ligand-targeted toxin conjugate (Tf-CRM107) for therapy of malignant gliomas. *Journal of neuro-oncology* **2003**, *65* (1), 3−13.

(14) Laske, D. W.; Youle, R. J.; Oldfield, E. H. Tumor regression with regional distribution of the targeted toxin TF-CRM107 in patients with malignant brain tumors. *Nature medicine* **1997**, *3* (12), 1362−1368.
(15) Kratz, F.; Beyer, U.; Roth, T.; Tarasova, N.; Collery, P.; Lechenault, F.; Cazabat, A.; Schumacher, P.; Unger, C.; Falken, U. Transferrin conjugates of doxorubicin: synthesis, characterization, cellular uptake, and in vitro efficacy. *Journal of pharmaceutical sciences* **1998**, *87* (3), 338−346.
(16) Goswami, U.; Dutta, A.; Raza, A.; Kandimalla, R.; Kalita, S.; Ghosh, S. S.; Chattopadhyay, A. Transferrin-Copper Nanocluster-Doxorubicin Nanoparticles as Targeted Theranostic Cancer Nanodrug. *ACS Appl. Mater. Interfaces* **2018**, *10* (4), 3282−3294.
(17) Szwed, M.; Laroche-Clary, A.; Robert, J.; Jozwiak, Z. Induction of apoptosis by doxorubicin-transferrin conjugate compared to free doxorubicin in the human leukemia cell lines. *Chemico-biological interactions* **2014**, *220*, 140−148.
(18) Nuhn, P.; De Bono, J. S.; Fizazi, K.; Freedland, S. J.; Grilli, M.; Kantoff, P. W.; Sonpavde, G.; Sternberg, C. N.; Yegnasubramanian, S.; Antonarakis, E. S. Update on Systemic Prostate Cancer Therapies: Management of Metastatic Castration-resistant Prostate Cancer in the Era of Precision Oncology. *European urology* **2019**, *75* (1), 88−99.
(19) Cucchiara, V.; Cooperberg, M. R.; Dall'Era, M.; Lin, D. W.; Montorsi, F.; Schalken, J. A.; Evans, C. P. Genomic Markers in Prostate Cancer Decision Making. *European urology* **2018**, *73* (4), 572−582.
(20) Haffner, M. C.; Zwart, W.; Roudier, M. P.; True, L. D.; Nelson, W. G.; Epstein, J. I.; De Marzo, A. M.; Nelson, P. S.; Yegnasubramanian, S. Genomic and phenotypic heterogeneity in prostate cancer. *Nature reviews. Urology* **2021**, *18* (2), 79−92.
(21) Donat, S. M.; Powell, C. T.; Israeli, R. S.; Fair, W. R.; Heston, W. D. Reversal by transferrin of growth-inhibitory effect of suramin on hormone-refractory human prostate cancer cells. *Journal of the National Cancer Institute* **1995**, *87* (1), 41−46.
(22) Zhao, Y.; Peng, J.; Yang, J.; Zhang, E.; Huang, L.; Yang, H.; Kakadiaris, E.; Li, J.; Yan, B.; Shang, Z.; et al. Enhancing Prostate-Cancer-Specific MRI by Genetic Amplified Nanoparticle Tumor Homing. *Advanced materials* **2019**, *31* (30), No. e1900928.
(23) de Kok, J. B.; Verhaegh, G. W.; Roelofs, R. W.; Hessels, D.; Kiemeney, L. A.; Aalders, T. W.; Swinkels, D. W.; Schalken, J. A. DD3(PCA3), a very sensitive and specific marker to detect prostate tumors. *Cancer Research* **2002**, *62* (9), 2695−2698.
(24) Pretlow, T. G.; Wolman, S. R.; Micale, M. A.; Pelley, R. J.; Kursh, E. D.; Resnick, M. I.; Bodner, D. R.; Jacobberger, J. W.; Delmoro, C. M.; Giaconia, J. M.; et al. Xenografts of primary human prostatic carcinoma. *Journal of the National Cancer Institute* **1993**, *85* (5), 394−398.
(25) Wang, Y.; Wang, H.; Li, C. Y.; Yuan, F. Effects of rate, volume, and dose of intratumoral infusion on virus dissemination in local gene delivery. *Molecular cancer therapeutics* **2006**, *5* (2), 362−366.
(26) Rossidis, A. C.; Stratigis, J. D.; Chadwick, A. C.; Hartman, H. A.; Ahn, N. J.; Li, H.; Singh, K.; Coons, B. E.; Li, L.; Lv, W.; et al. In utero CRISPR-mediated therapeutic editing of metabolic genes. *Nature medicine* **2018**, *24* (10), 1513−1518.
(27) Khare, R.; Chen, C. Y.; Weaver, E. A.; Barry, M. A. Advances and future challenges in adenoviral vector pharmacology and targeting. *Current gene therapy* **2011**, *11* (4), 241−258.
(28) Lang, F. F.; Conrad, C.; Gomez-Manzano, C.; Yung, W. K. A.; Sawaya, R.; Weinberg, J. S.; Prabhu, S. S.; Rao, G.; Fuller, G. N.; Aldape, K. D.; et al. Phase I Study of DNX-2401 (Delta-24-RGD) Oncolytic Adenovirus: Replication and Immunotherapeutic Effects in Recurrent Malignant Glioma. *Journal of clinical oncology: official journal of the American Society of Clinical Oncology* **2018**, *36* (14), 1419−1427.

https://doi.org/10.1021/acs.nanolett.2c00931
Nano Lett. XXXX, XXX, XXX−XXX